



## Separation of alumina and silica from metakaolinite by reduction roasting–alkaline leaching process: Effect of $\text{CaSO}_4$ and $\text{CaO}$

Hong-yang WANG<sup>1,2</sup>, Xiao-xue ZHANG<sup>1</sup>, Si-yuan YANG<sup>1,2</sup>, Cheng LIU<sup>1,2</sup>, Li-qun LUO<sup>1,2</sup>

1. School of Resources and Environmental Engineering, Wuhan University of Technology, Wuhan 430070, China;

2. Hubei Key Laboratory of Mineral Resources Processing and Environment,

Wuhan University of Technology, Wuhan 430070, China

Received 8 February 2021; accepted 20 October 2021

**Abstract:** Limestone ( $\text{CaCO}_3$ ), which could promote sulfur fixation, was added to coal gangue during roasting in a circulating fluidized bed (CFB) boiler.  $\text{CaO}$  and  $\text{CaSO}_4$  were the main Ca-bearing minerals while metakaolinite was the major Al-bearing mineral in CFB slag. The effect of  $\text{CaSO}_4$  and  $\text{CaO}$  on the separation of alumina and silica from metakaolinite by reduction roasting–alkaline leaching process was studied. Results showed that metakaolinite was completely converted into hercynite and silica solid solutions (i.e., quartz and cristobalite solid solutions) by reduction roasting with hematite. More than 95% of silica in the reduced specimen was removed by alkaline leaching. The addition of  $\text{CaSO}_4$  and  $\text{CaO}$  remarkably decreased the separation efficiency of alumina and silica in metakaolinite, which could be attributed to the formation of Si-bearing minerals: (1) Fayalite and anorthite were formed during the reduction roasting process; (2) Fayalite was stable while anorthite was converted into sodalite and wollastonite during the alkaline leaching process. This study demonstrates that sulfur in coal gangue should be fixed by treating the exhaust gas instead of controlling the combustion process of CFB to achieve the comprehensive recovery of silica and alumina from the CFB slag.

**Key words:** circulating fluidized bed slag; metakaolinite; Ca-bearing minerals; reduction roasting; alkaline leaching

### 1 Introduction

Nowadays, coal is still the primary energy resource in China due to the shortage of oil and gas. During coal mining and washing, approximately 10%–15% of the total coal production is discarded in the form of coal gangue [1]. Therefore, coal gangue is one of the largest forms of industrial solid wastes. Indeed, its stockpile occupies large quantities of farmland and causes severe pollution to the surrounding environment [2,3]. The comprehensive utilization of coal gangue in the industry includes land reclamation [4] and building materials [5]. Commercial heat and electricity may

also be generated by burning coal gangue with a circulating fluidized bed (CFB) boiler at 800–900 °C [6]. Limestone ( $\text{CaCO}_3$ ), which is usually added to the CFB boiler, can fix the sulfur from coal gangue through the formation of  $\text{CaSO}_4$ . The Ca-bearing minerals of  $\text{CaO}$  and  $\text{CaSO}_4$  can be found in the CFB slag [7].

CFB slag is a raw material with potential use in building materials, such as brick, cement, and ceramic [8–10]. Over 80% of the coal in China is mainly distributed in northern and western regions, but the main cities are located at the center and east of the country. Therefore, the large-scale consumption of CFB slag cannot be achieved through producing building materials, which have

**Corresponding author:** Si-yuan YANG, Tel: +86-13294166556, E-mail: [siyuan.yang@whut.edu.cn](mailto:siyuan.yang@whut.edu.cn);

Cheng LIU, Tel: +86-13928981935, E-mail: [145601011@csu.edu.cn](mailto:145601011@csu.edu.cn)

DOI: 10.1016/S1003-6326(22)65849-7

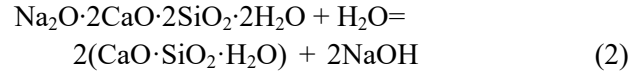
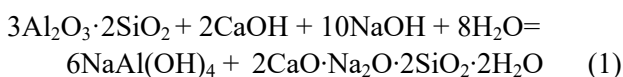
1003-6326/© 2022 The Nonferrous Metals Society of China. Published by Elsevier Ltd & Science Press

the characteristic of limited transportation distance due to the low value. Considering that CFB slag contains 25%–45% alumina, which mainly exists in the form of metakaolinite, alumina extraction may present an efficient approach for the high-value application [11].

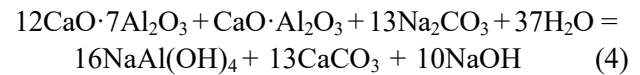
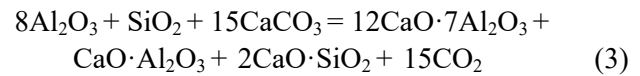
Acid leaching and alkaline leaching are the main methods to extract alumina from CFB slag owing to the dissolution performance of alumina. In the acid leaching process, alumina enters the solution in the form of Al ions, while silica is stable and abandoned in the leaching residue [12,13]. However, the Fe/Mg-bearing minerals in CFB slag also react with the acid solution, resulting in poor solution purification. The generation of waste acid water and the requirement of corrosion-resistant equipment are also the drawbacks of acid leaching process.

The alkaline leaching process can be classified into hydrothermal and sintering processes. The hydrothermal process is focused on the alumina extraction by digesting CFB slag in NaOH solution ( $\text{Na}_2\text{O}$ : 300–400 g/L) at 260–300 °C, after which the silica is converted into solid  $\text{NaCaHSiO}_4$ , as shown in Eq. (1).  $\text{NaCaHSiO}_4$  is unstable in NaOH solution ( $\text{Na}_2\text{O}$ : <100 g/L) at 90–120 °C, and decomposed into  $\text{CaSiO}_3 \cdot \text{H}_2\text{O}$  and NaOH, as shown in Eq. (2) [14,15]. Therefore, the main mineral in red mud is  $\text{CaSiO}_3 \cdot \text{H}_2\text{O}$ . When sintering with lime, alumina in CFB slag is transformed into  $12\text{CaO} \cdot 7\text{Al}_2\text{O}_3$  and  $\text{CaO} \cdot \text{Al}_2\text{O}_3$ , and meanwhile the silica is converted into stable  $2\text{CaO} \cdot \text{SiO}_2$  [16,17]. Alumina in the sintering product can be recovered by leaching with  $\text{Na}_2\text{CO}_3$  solution, and  $2\text{CaO} \cdot \text{SiO}_2$  and  $\text{CaCO}_3$  are the main minerals in red mud. This method is known as the lime-sintering process, the reactions for which are presented in Eqs. (3) and (4). Another typical sintering process is the lime-soda sintering process. After sintering with CaO and  $\text{Na}_2\text{CO}_3$ , alumina in CFB slag is converted into  $\text{NaAlO}_2$ , while silica is converted into  $2\text{CaO} \cdot \text{SiO}_2$  [18,19]. The separation of alumina and silica from the sintering product can be achieved by leaching with water or dilute NaOH solution. The reactions of the lime-soda sintering process are shown in Eqs. (5) and (6).

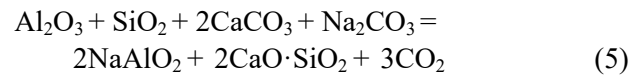
Hydrothermal process:



Lime sintering process:



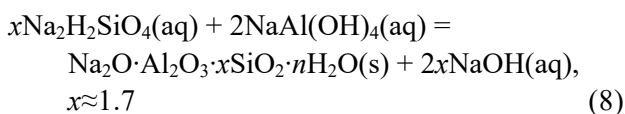
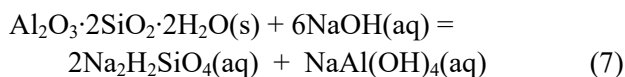
Lime-soda sintering process:



The core issue in alumina extraction from CFB slag by the alkaline process is to convert alumina into a solution with or without pretreatment, while silica is converted into stable Si–Ca compounds. If the mass ratio of alumina to silica (A/S) in CFB slag is ~1.0, the output of red mud can be calculated according to the reactions given in Eqs. (1)–(6). The highest output of red mud (4.0–5.5 t/t( $\text{Al}_2\text{O}_3$ )) is achieved by the lime-soda sintering process because the main minerals in red mud are  $2\text{CaO} \cdot \text{SiO}_2$  and  $\text{CaCO}_3$ . Approximately 3.0 t of red mud is produced for every ton of alumina production by hydrothermal process or lime-soda sintering process. In addition, the large-scale utilization of red mud remains a global problem due to its complex composition, large specific surface area, and strong alkalinity [20]. Thus, the alkaline leaching process described above is unsuitable for treating the CFB slag.

Bayer process is the primary method to extract alumina from bauxite in the world [21]. In many modern alumina plants, a predestination stage, during which the slurry of bauxite and sodium aluminate solution is kept at ~95 °C for several hours, is conducted to convert the silica into solid desilication products, as shown in Eqs. (7) and (8) [22,23]. According to these reactions, about 1.0 t  $\text{Al}_2\text{O}_3$  and 0.6 t  $\text{Na}_2\text{O}$  per 1.0 t  $\text{SiO}_2$  are irrevocably lost to red mud. Thus, the alumina in CFB slag cannot be extracted directly by the Bayer process because of the low A/S (i.e., ~1.0). If the silica in CFB slag is removed by alkaline leaching, the alumina in the leaching residue can be extracted by the Bayer process. Unfortunately, the traditional roasting-leaching process cannot realize the efficient separation of silica and alumina from kaolinite because of the formation of  $3\text{Al}_2\text{O}_3 \cdot 2\text{SiO}_2$

spinel during roasting [24].



To decompose the Al—O—Si bond in kaolinite completely, researchers have proposed the conversion of kaolinite into hercynite and silica solid solutions (i.e., quartz solid solution (QSS) and cristobalite solid solution (CSS)) through reduction roasting with hematite. The efficient separation of silica and alumina in the reduced specimen can be realized by leaching with NaOH solution at ~110 °C. After pre-oxidation roasting, the alumina in hercynite can be extracted by the Bayer process, and hematite in the red mud can be recycled by physical separation [24–27]. Therefore, the red mud generation of this novel technology is small because of the comprehensive recovery of silica and alumina together with the recycling of hematite. However, previous studies were only focused on the kaolin and simulated CFB slag. The effect of Ca-bearing minerals (i.e., CaSO<sub>4</sub> and CaO) on the separation of silica and alumina was neglected during the reduction roasting–alkaline leaching process for CFB slag treatment.

In this study, the phase transformations observed during the reduction roasting of a mixture of metakaolin and hematite in the absence and presence of CaSO<sub>4</sub> and CaO were investigated by X-ray diffraction (XRD). The separation of silica and alumina in the reduced specimens was then carried out by leaching with NaOH solution. The leaching residue was analyzed by X-ray photoelectron spectroscopy (XPS), scanning electron microscopy (SEM), and energy dispersive spectrometry (EDS) to assess the role of CaSO<sub>4</sub> and CaO in the separation of silica and alumina from metakaolinite.

## 2 Experimental

### 2.1 Materials

NaOH solution was prepared by dissolving analytically pure NaOH (≥96.00%) in deionized water. The proximate analysis of coal powder used as a reducing agent in this work showed fixed carbon, volatile matters, and ash contents of

80.78%, 9.04% and 9.08%, respectively. Hematite (Fe<sub>2</sub>O<sub>3</sub> ≥99.00%) used during reduction roasting was analytically pure, and metakaolin was obtained by roasting kaolin in air at 850 °C for 60 min. The chemical compositions of the kaolin and metakaolin in this work are listed in Table 1. The kaolin was composed of 37.69% Al<sub>2</sub>O<sub>3</sub> and 44.61% SiO<sub>2</sub>, and the Al<sub>2</sub>O<sub>3</sub> and SiO<sub>2</sub> contents in metakaolin increased to 43.68% and 51.12% due to the dehydration.

**Table 1** Chemical compositions of kaolin and metakaolin (wt.%)

Sample	Al <sub>2</sub> O <sub>3</sub>	SiO <sub>2</sub>	TiO <sub>2</sub>	Fe <sub>2</sub> O <sub>3</sub>	CaO	A/S
Kaolin	37.69	44.61	1.24	0.26	0.08	0.84
Metakaolin	43.68	51.12	1.42	0.42	0.11	0.85

Metakaolin was obtained by roasting the kaolin in the air at 850 °C for 60 min

### 2.2 Procedures

Metakaolin, hematite, and coal powder with Fe<sub>2</sub>O<sub>3</sub>/Al<sub>2</sub>O<sub>3</sub>/C molar ratio of 1.2:2.0:1.2 were well mixed by a vibrating mill for 2 min. CaSO<sub>4</sub> and CaO was added at a rate 5% of the metakaolin content to investigate the effect of Ca-bearing minerals on the separation of alumina and silica during the reduction roasting–alkaline leaching process. The reduction roasting experiments were conducted in a muffle furnace (SX2–8–16, Shanghai Kunchengkeyi Co., Ltd., China) at 1100 °C for 30, 60, and 90 min. The detailed experimental process was described in an earlier study [25]. The reduced specimens obtained without CaSO<sub>4</sub> and CaO additive were designated as reduced metakaolinite (RM), while those obtained with CaSO<sub>4</sub> and CaO as additives were designated as RM-CaSO<sub>4</sub> and RM-CaO, respectively.

The alkaline leaching experiments were conducted on a GS–0.25 autoclave (Weihai Dingda Chemical Machinery Co., Ltd., China). 10 g of the reduced specimen with particle size of <74 μm and 100 mL of a solution with a NaOH concentration of 160 g/L were placed into the autoclave. The autoclave was then heated to 110 °C and maintained at that temperature for 120 min. After that, the autoclave was opened until the temperature decreased to 70 °C by cooling with tap water. The slurry was treated by liquid–solid separation, and the obtained solid was used for analysis after drying in an oven for 5 h.

### 2.3 Analysis methods

Thermogravimetric analysis of kaolin was carried out by SDTQ600 thermal analyzer (TA, USA). Phase analyses of the reduced specimens and their leaching residues were performed by XRD (MAX-RB, Rigaku Co., Japan). The leaching residues of RM-CaSO<sub>4</sub> and RM-CaO were analyzed by XPS (ESCALAB 250XI, Thermo Fisher Scientific, USA). SEM (JSM-6360LV, JEOL, Japan) and EDX (GENESIS60S, EDAX, USA) were respectively conducted to analyze the microscopic surface morphology and micro area composition. The chemical compositions of reduced specimens and their leaching residues were analyzed by a CONTRAA-700 atomic absorption spectrometer (Analytik Jena AG, Germany). The silica leaching ratio was calculated using Eq. (9):

$$R = \left(1 - \frac{c_b m_b}{c_a m_a}\right) \times 100\% \quad (9)$$

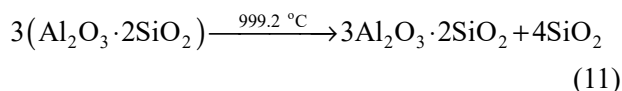
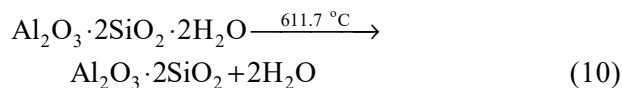
where  $R$  is the silica leaching ratio, %;  $c_b$  is the silica content in leaching residue, %;  $m_b$  is the mass of leaching residue, g;  $c_a$  is the silica content in reduced specimen, %;  $m_a$  is the mass of reduced specimen, g.

## 3 Results and discussion

### 3.1 Phase transformation of kaolinite during roasting

The thermogravimetric analysis results of kaolin are shown in Fig. 1. A slight mass loss of kaolin was revealed at 25–100 °C. The mass loss rate of the kaolin then increased with increasing temperature and reached 13.81% at ~700 °C. Two

peaks at 67.6 and 563.3 °C were observed on the DTG curve, indicating the rapid mass loss at these temperatures. On the DSC curve, two endothermic peaks at 85.9 and 611.7 °C and an exothermic peak at 999.2 °C were observed. The first endothermic peak at 85.9 °C could be attributed to the removal of molecular water in kaolin, while the second endothermic peak at 611.7 °C could be caused by the dehydration of kaolinite, as shown in Eq. (10). No significant changes in mass were observed as the temperature continued to increase to 999.2 °C, but an exothermic peak was observed due to the conversion of metakaolinite into crystallized mullite as indicated in Eq. (11). Therefore, metakaolinite was the stable product of kaolinite decomposed at 700–900 °C.



The XRD patterns of kaolin and metakaolin are shown in Fig. 2. Figure 2(a) shows that the composition of kaolin was relatively simple because only kaolinite could be detected in the XRD pattern. Figure 2(b) reveals the disappearance of diffraction peaks of kaolinite and the generation of a non-crystal diffraction peak in the  $2\theta$  range of 15°–30° after roasting at 850 °C for 60 min. This finding indicates that metakaolinite was a typical amorphous phase. Weak peaks of quartz were also found in the XRD pattern of metakaolin (Fig. 2(b)), meaning that the kaolin contained a small amount of quartz.

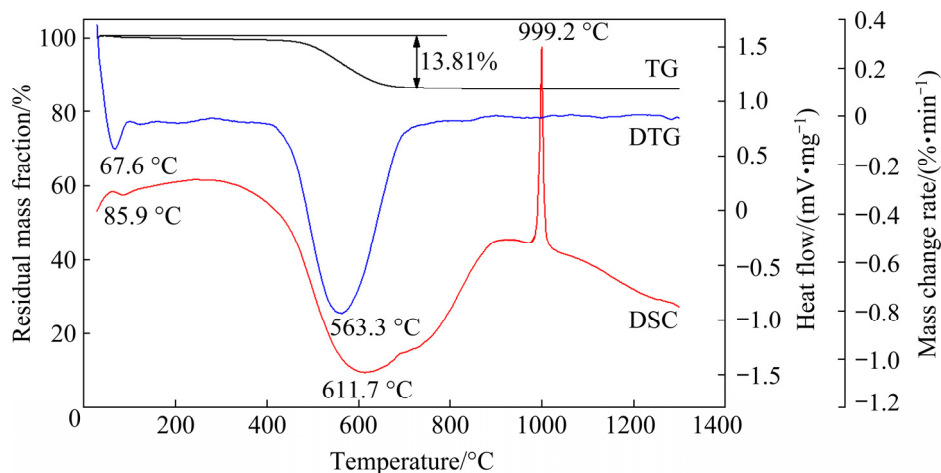


Fig. 1 Thermogravimetric analysis results of kaolin

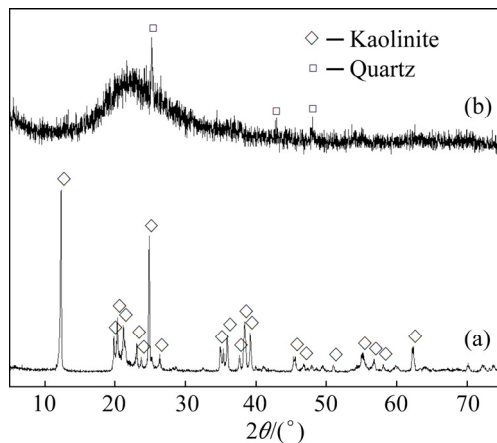


Fig. 2 XRD patterns of kaolin (a) and metakaolin (b)

### 3.2 Effect of $\text{CaSO}_4$ and $\text{CaO}$ on reactions during reduction roasting

The XRD patterns of specimens reduced at  $1100\text{ }^\circ\text{C}$  are presented in Fig. 3. Figure 3(a) shows that hercynite, cristobalite and quartz were the main minerals in RM. In this work, the cristobalite and quartz found in RM were considered CSS and QSS because of their ready solubility in NaOH solution [24]. Figure 3(a) also reveals the increase in the diffraction peaks of CSS and the decrease in those of QSS, indicating that prolonging the roasting time could facilitate the conversion of QSS into CSS. Except for hercynite and CSS, fayalite ( $2\text{FeO}\cdot\text{SiO}_2$ ) and anorthite ( $\text{CaO}\cdot\text{Al}_2\text{O}_3\cdot 2\text{SiO}_2$ ) were also found in Fig. 3(b). During the reduction roasting at  $1100\text{ }^\circ\text{C}$ ,  $\text{CaSO}_4$  could be decomposed into  $\text{CaO}$  and  $\text{SO}_2$  with the presence of carbon [28]. Anorthite was then formed through the reaction between  $\text{CaO}$  and metakaolinite. The excessive hematite could react with silica solid solutions to generate fayalite during the reduction roasting, as verified by the decrease in the XRD peaks of CSS. The comparison of Fig. 3(b) with Fig. 3(c) demonstrates that the addition of  $\text{CaO}$  could promote the formation of anorthite and fayalite. The XRD peak of QSS disappeared in Figs. 3(b, c), indicating that the presence of  $\text{CaSO}_4$  and  $\text{CaO}$  could promote the conversion of QSS into CSS.

### 3.3 Separation of alumina and silica by alkaline leaching

The silica leaching ratio and the A/S in leaching residue of the reduced specimens are shown in Fig. 4. When the roasting time was prolonged from 30 to 90 min, the silica leaching

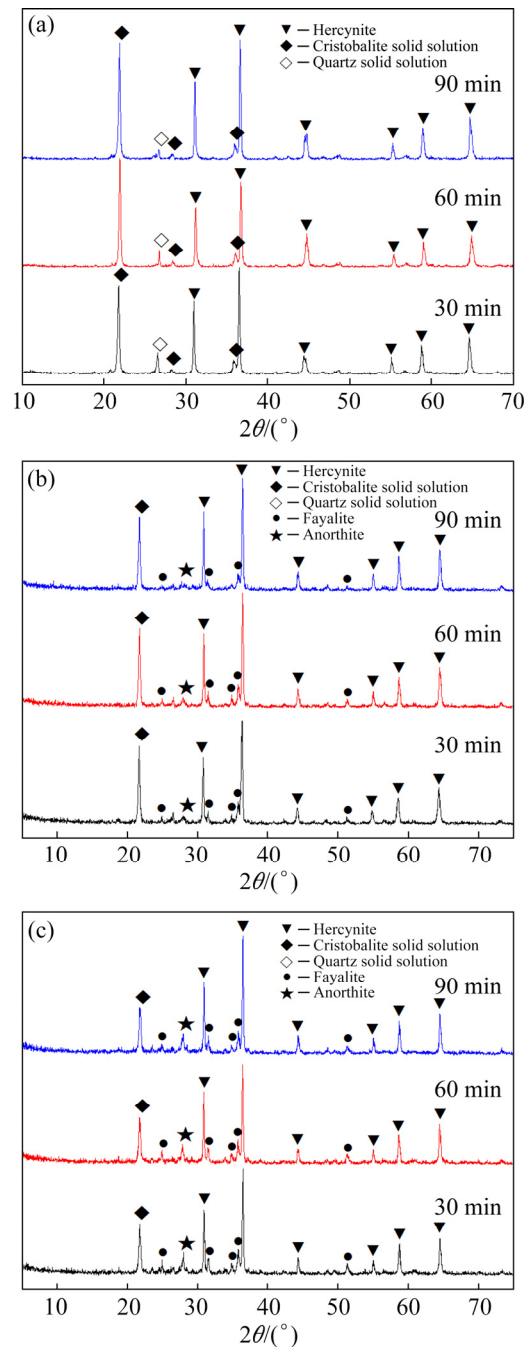
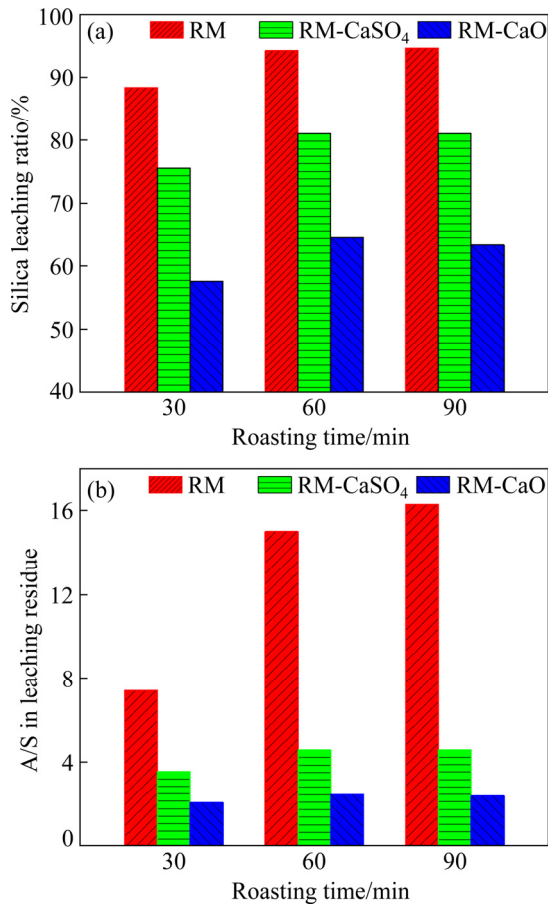


Fig. 3 XRD patterns of specimens reduced at  $1100\text{ }^\circ\text{C}$ : (a) RM; (b) RM- $\text{CaSO}_4$ ; (c) RM- $\text{CaO}$

ratio of RM increased from 88.37% to 94.70% and the corresponding A/S in leaching residue rose from 7.44 to 16.32. The increase of roasting time could promote the conversion of metakaolinite into hercynite and silica solid solutions during reduction roasting with hematite, which leads to an increase in silica leaching ratio. Compared with the leaching results of RM, the silica leaching ratio and A/S in leaching residue of RM- $\text{CaSO}_4$  revealed a significant decrease, which may be attributed to the



**Fig. 4** Silica leaching ratio of reduced specimen (a) and A/S in leaching residue (b) (Leaching conditions: 110 °C, 120 min, 160 g/L of NaOH, 10:1 of liquid/solid ratio)

formation of fayalite, as presented in Fig. 3(b). Among the specimens analyzed, RM-CaO revealed the lowest silica leaching ratio and A/S in leaching residue, at 63.39% and 2.36, respectively. Thus, the addition of CaSO<sub>4</sub> and CaO during the reduction roasting could reduce the silica leaching ratio from the reduced specimens by NaOH solution leaching. In this case, the Bayer process cannot extract the alumina in the obtained residues with low A/S.

The XRD patterns of the leaching residues of the reduced specimens are shown in Fig. 5. Comparison of Fig. 5 with Fig. 3 reveals the disappearance of the XRD peaks of QSS and CSS after alkaline leaching, indicating that both QSS and CSS were efficiently dissolved into NaOH solution. By contrast, hercynite appeared to be stable in NaOH solution under the leaching conditions employed in this work on account of its normal spinel structure [27].

Figure 5(a) reveals the presence of sodalite in the leaching residue of RM roasted for 30 min.

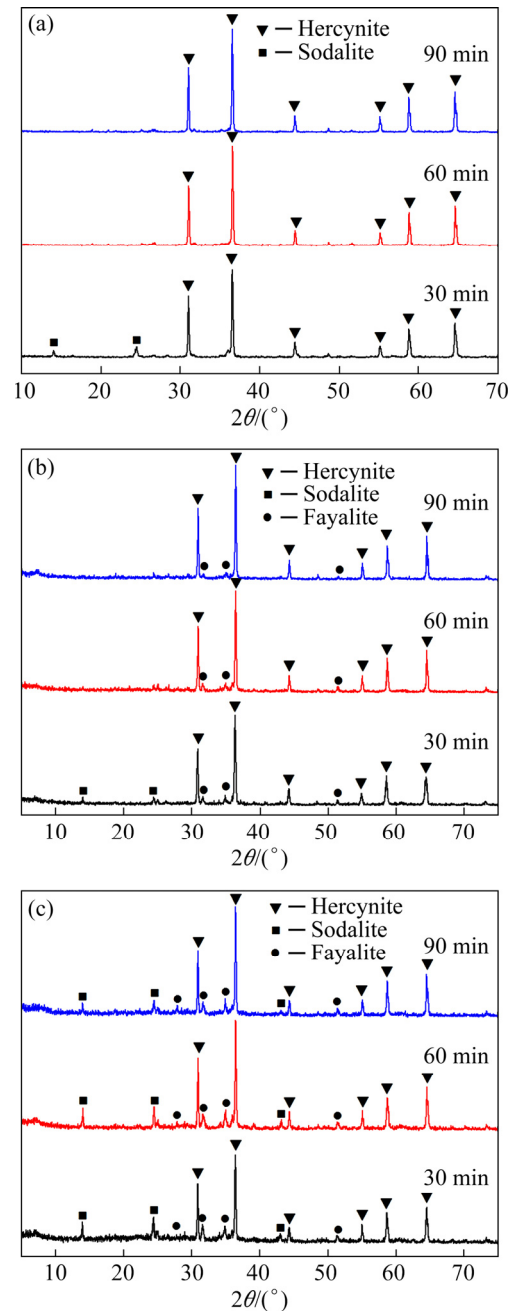
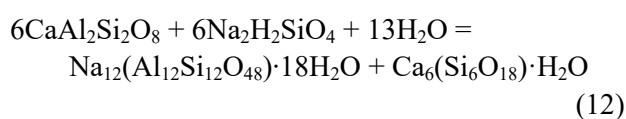


**Fig. 5** XRD patterns of leaching residues: (a) RM; (b) RM-CaSO<sub>4</sub>; (c) RM-CaO (Leaching conditions: 110 °C, 120 min, 160 g/L of NaOH, 10:1 of liquid/solid ratio)

When a mixture of metakaolin, hematite and coal powder was roasted at 1100 °C for 30 min, the unreacted metakaolinite decomposed into amorphous mullite and silica. Thereafter, the amorphous mullite reacted with NaOH solution to produce sodalite during alkaline leaching. Figure 5(a) also shows that metakaolinite could efficiently react with hematite during reduction roasting at 1100 °C for 60–90 min. Besides

hercynite and sodalite, fayalite was also detected in the leaching residues of RM-CaSO<sub>4</sub> and RM-CaO, as shown in Figs. 5(b, c), thereby indicating that fayalite was stable in NaOH solution. Comparison of Fig. 5(c) with Fig. 3(c) reveals the disappearance of the XRD peaks of anorthite after alkaline leaching, indicating the reaction of anorthite with NaOH solution to form sodalite. However, Ca-bearing minerals were not found in the leaching residues of RM-CaSO<sub>4</sub> and RM-CaO, and these amorphous minerals might exist in the leaching residues.

The leaching residues of RM-CaSO<sub>4</sub> and RM-CaO obtained by reductively roasting at 1100 °C for 60 min were analyzed by XPS, and the results are presented in Fig. 6. The main Si-bearing minerals in leaching residues were sodalite and wollastonite. By combining the results in Fig. 6 with the phase transformation shown in Fig. 3 and Fig. 5, anorthite could be inferred to react with the alkaline silicate solution to produce sodalite and wollastonite during the leaching process, as presented in Eq. (12):



Therefore, the presence of CaSO<sub>4</sub> and CaO could remarkably reduce the separation efficiency of alumina and silica from metakaolinite by reduction roasting–alkaline leaching process, due to the formation of fayalite during reduction roasting and the generation of sodalite and wollastonite during alkaline leaching.

### 3.4 Morphology of reduced specimens and leaching residues

The SEM–EDS results of RM obtained by roasting for 60 min and its leaching residue are shown in Fig. 7. The obtained RM had a loose structure and could be easily ground into fine particles. Figure 7(a) shows that Fe, Al and Si were well dispersed in the RM, and a small amount of unreacted metakaolinite (marked by the red circle) was also detected. Thus, metakaolinite could efficiently react with hematite during the reduction roasting process, but the independent particles of hercynite and silica were not generated in the RM. Figure 7(b) shows that the leaching residue had a porous structure after alkaline leaching of silica. The distribution of Fe was consistent with that of Al

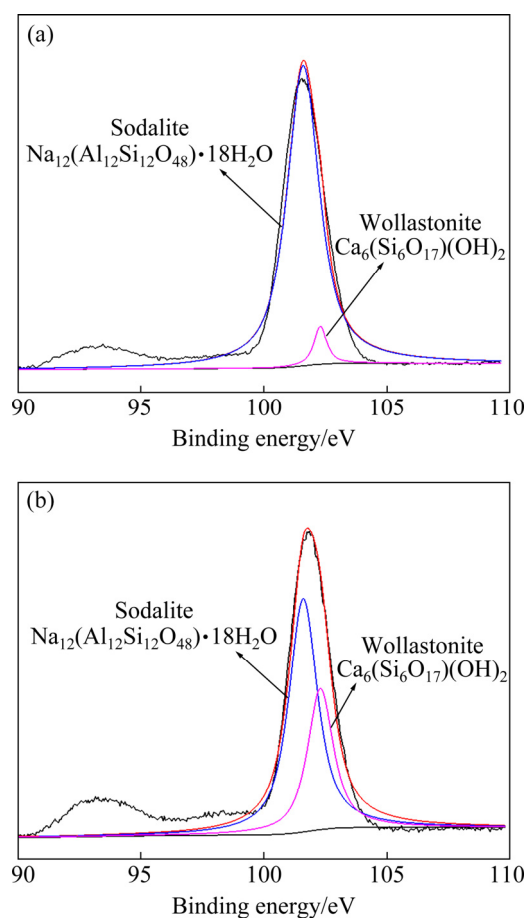


**Fig. 6** Si 2p XPS spectra of leaching residues: (a) RM-CaSO<sub>4</sub>; (b) RM-CaO (Leaching conditions: 110 °C, 120 min, 160 g/L of NaOH, 10:1 of liquid/solid ratio)

in the leaching residue, but the silica content clearly decreased. Therefore, QSS and CSS in RM could be dissolved into NaOH solution, whereas the stable hercynite was enriched in the leaching residue.

The SEM–EDS results of RM-CaSO<sub>4</sub> roasted for 60 min and its leaching residue are shown in Fig. 8. The comparison of Fig. 8(a) with Fig. 7(a) reveals that addition of CaSO<sub>4</sub> had no significant effect on RM-CaSO<sub>4</sub>, which had a loose structure. Ca was distributed in a simple manner in RM-CaSO<sub>4</sub> with Al and Si. Therefore, CaSO<sub>4</sub> was unstable during the reduction roasting process, and its decomposition product (CaO) could react with metakaolinite to form anorthite (Fig. 3(b)). Figure 8(b) indicates that the distribution of Fe was similar to that of Al, but Ca and Si were mainly distributed on the particle surface in the leaching residue. During alkaline leaching, hercynite was stable and enriched in the leaching residue. However, the CSS in RM-CaSO<sub>4</sub> was dissolved into

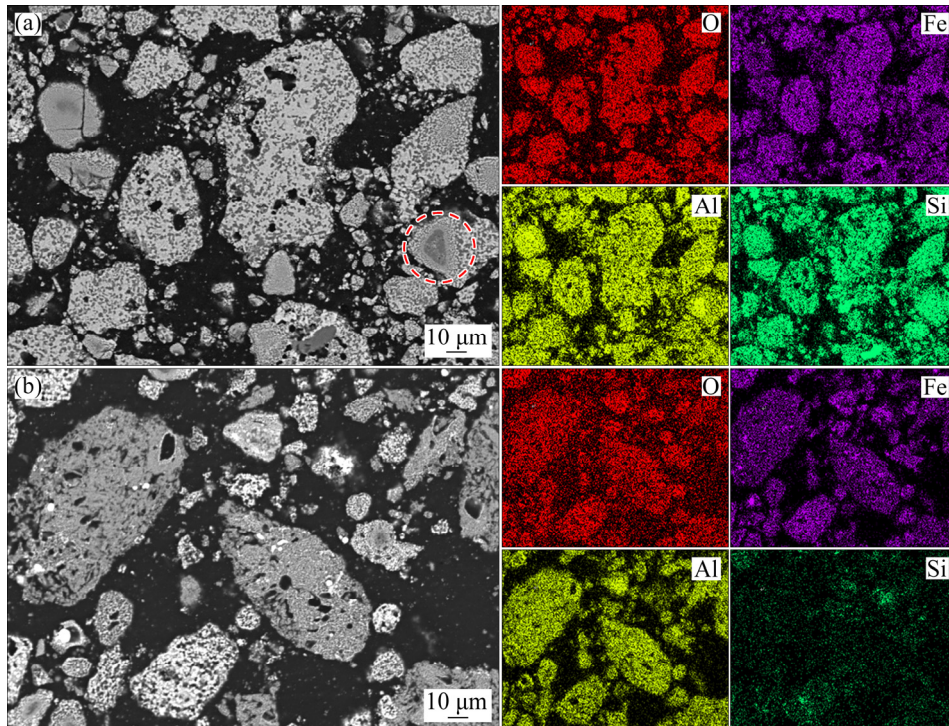


**Fig. 7** SEM-EDS results of RM roasted for 60 min (a) and its leaching residue (b)

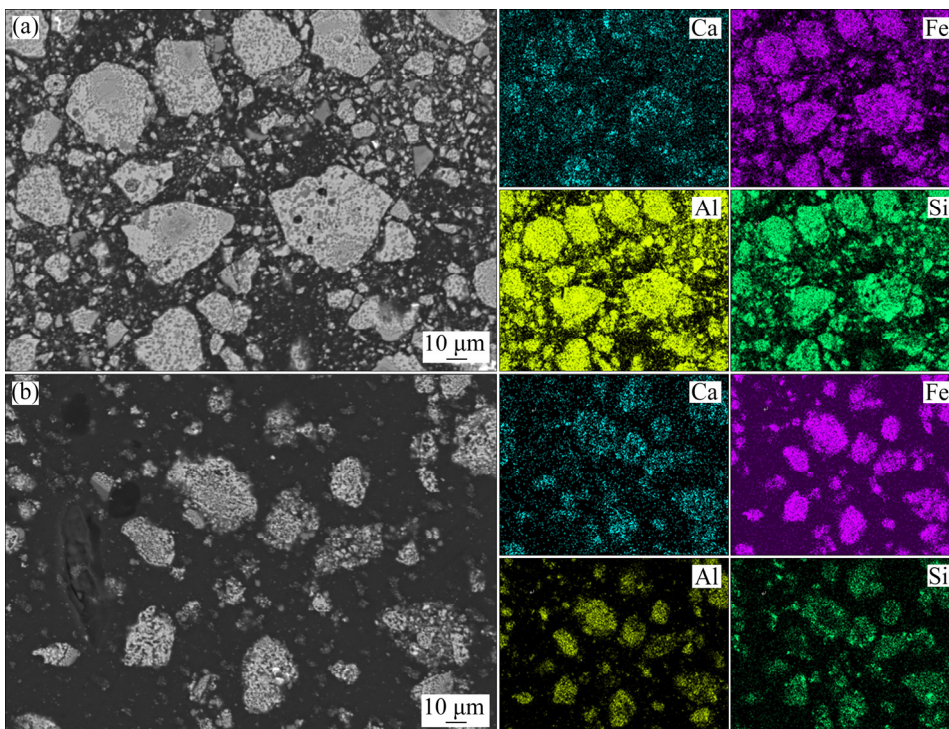


**Fig. 8** SEM-EDS results of RM-CaSO<sub>4</sub> roasted for 60 min (a) and its leaching residue (b)

NaOH solution, and the Ca-bearing mineral of anorthite was converted into sodalite and wollastonite, as found in Fig. 6(a). Therefore, the new products of sodalite and wollastonite could be enriched on the particle surface of hercynite.

Figure 9 shows the SEM-EDS results of RM-CaO roasted for 60 min and its leaching residue. The obtained RM-CaO had a dense structure and was difficult to break. Ca, Al and Si were evenly distributed in the RM-CaO, but the

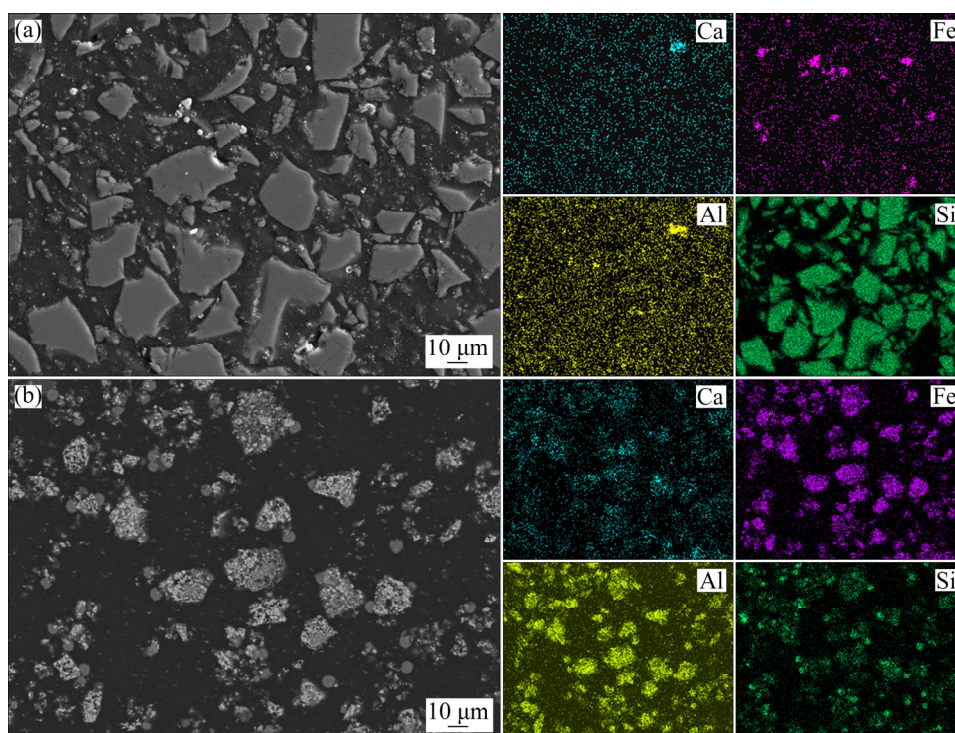


**Fig. 9** SEM-EDS results of RM-CaO roasted for 60 min (a) and its leaching residue (b)

independent Fe-bearing mineral (i.e., metallic iron) could be found in Fig. 9(a). Thus, the reaction between CaO and metakaolinite occurred prior to that between  $\text{Fe}_2\text{O}_3$  and metakaolinite during the reduction roasting, and the unreacted  $\text{Fe}_2\text{O}_3$  was reduced into metallic iron. Figure 9(b) reveals that Si was mainly enriched in the fine particles of the leaching residue, while Ca was distributed on the particle surface. During the alkaline leaching, sodalite and wollastonite, generated from the reaction between anorthite and alkaline silicate solution, could be absorbed on the hercynite particle surface.

Overall, the presence of  $\text{CaSO}_4$  and CaO in the CFB slag could remarkably decrease the separation efficiency of alumina and silica from metakaolinite during reduction roasting–alkaline leaching process. The alumina in the leaching residue was difficult to extract by Bayer digestion because of the low A/S, and hematite added to the system was difficult to recycle. Thus, addition of limestone should be avoided when treating the coal gangue by a CFB boiler. Sulfur fixation could be achieved by treating the boiler fuel gas. Ultimately, the high-value application of CFB slag was realized through the comprehensive recovery of silica and alumina based on the recycle of hematite.

## 4 Conclusions

(1) The efficient separation of silica and alumina from metakaolinite was achieved. First, metakaolinite was converted into hercynite and silica solid solutions by reduction roasting with hematite. Thereafter, the silica solid solutions were removed by NaOH solution leaching, and the stable hercynite was enriched in the leaching residue.

(2) During reduction roasting,  $\text{CaSO}_4$  and CaO additive could react with metakaolinite to form anorthite, and the excessive hematite was combined with the silica solid solutions to generate fayalite. The obtained RM-CaO had a dense structure.

(3) During the alkaline leaching of silica, fayalite was stable in NaOH solution and enriched in the leaching residue, while anorthite could react with the alkaline silicate solution to produce sodalite and wollastonite. These processes led to the decreased separation efficiency of silica and alumina from metakaolinite.

## Acknowledgments

The authors are grateful for the financial supports from the National Natural Science Foundation of China (Nos. 52004194, 51874219),

and the China Postdoctoral Science Foundation (No. 2019M662733).

## References

- [1] LI Jia-yan, WANG Jin-man. Comprehensive utilization and environmental risks of coal gangue: A review [J]. *Journal of Cleaner Production*, 2019, 239: 117946.
- [2] QIN Ling, GAO Xiao-jian. Properties of coal gangue–Portland cement mixture with carbonation [J]. *Fuel*, 2019, 245: 1–12.
- [3] XIE Ming-zhuang, LIU Feng-qin, ZHAO Hong-liang, KE Chao-yang, XU Zhi-qian. Mineral phase transformation in coal gangue by high temperature calcination and high-efficiency separation of alumina and silica minerals [J]. *Journal of Materials Research and Technology*, 2021, 14: 2281–2288.
- [4] JABŁOŃSKA B, KITYK A V, BUSCH M, HUBER P. The structural and surface properties of natural and modified coal gangue [J]. *Journal of Environmental Management*, 2017, 190: 80–90.
- [5] HUANG Guo-dong, JI Yong-sheng, LI Jun, HOU Zhi-hui, DONG Zuo-chao. Improving strength of calcinated coal gangue geopolymer mortars via increasing calcium content [J]. *Construction and Building Materials*, 2018, 166: 760–768.
- [6] ZHAO Li-zheng, DU Yan-fei, ZENG Yu-sen, KANG Zhi-zhong, SUN Bao-min. Sulfur conversion of mixed coal and gangue during combustion in a CFB boiler [J]. *Energies*, 2020, 13(3): 553.
- [7] ZHANG Wen-yan, CHOI H, SAGAWA T, HAMA Y. Compressive strength development and durability of an environmental load-reduction material manufactured using circulating fluidized bed ash and blast-furnace slag [J]. *Construction and Building Materials*, 2017, 146: 102–113.
- [8] KUZ'MIN M P, LARIONOV L M, KONDRATIEV V V, KUZ'MINA M Y, GRIGORIEV V G, KUZ'MINA A S. Use of the burnt rock of coal deposits slag heaps in the concrete products manufacturing [J]. *Construction and Building Materials*, 2018, 179: 117–124.
- [9] QIU Rui-fang, CHENG Fang-qin, HUANG Hai-ming. Removal of Cd<sup>2+</sup> from aqueous solution using hydrothermally modified circulating fluidized bed fly ash resulting from coal gangue power plant [J]. *Journal of Cleaner Production*, 2018, 172: 1918–1927.
- [10] HE Pan-yang, ZHANG Yao-jun, CHEN Hao, HAN Zhi-chao, LIU Li-cai. Low-energy synthesis of kaliophilite catalyst from circulating fluidized bed fly ash for biodiesel production [J]. *Fuel*, 2019, 257: 116041
- [11] XIAO Jin, LI Fa-chuang, ZHONG Qi-fan, BAO Hong-guang, WANG Bing-jie, HUANG Jin-di, ZHANG Yan-bing. Separation of aluminum and silica from coal gangue by elevated temperature acid leaching for the preparation of alumina and SiC [J]. *Hydrometallurgy*, 2015, 155: 118–124.
- [12] TRIPATHY A K, BEHERA B, AISHVARYA V, SHEIK A R, DASH B, SARANGI C K, TRIPATHY B C, SANJAY K, BHATTACHARYA I N. Sodium fluoride assisted acid leaching of coal fly ash for the extraction of alumina [J]. *Minerals Engineering*, 2019, 131(15): 140–145.
- [13] GUO Yan-xia, YAN Ke-zhou, CUI Li, CHENG Fang-qin. Improved extraction of alumina from coal gangue by surface mechanically grinding modification [J]. *Powder Technology*, 2016, 302: 33–41.
- [14] ZHANG Ran, MA Shu-hua, YANG Quan-cheng, ZHENG Shi-li, ZHANG Yi, KIM N, HONG S. Research on NaCaHSiO<sub>4</sub> decomposition in sodium hydroxide solution [J]. *Hydrometallurgy*, 2011, 108: 205–213.
- [15] DING Jian, MA Shu-hua, ZHENG Shi-li, ZHANG Yi, XIE Zong-li, SHEN S, LIU Zhong-kai. Study of extracting alumina from high-alumina PC fly ash by a hydro-chemical process [J]. *Hydrometallurgy*, 2016, 161: 58–64.
- [16] MATJIE R H, BUNT J R, van HEERDEN J H P. Extraction of alumina from coal fly ash generated from a selected low rank bituminous South African coal [J]. *Minerals Engineering*, 2005, 18(3): 299–310.
- [17] EIDEEB A B, BRICHKIN V N, BERTAU M, SAVINOVA Y A, KURTENKOV R V. Solid state and phase transformation mechanism of kaolin sintered with limestone for alumina extraction [J]. *Applied Clay Science*, 2020, 196: 105771.
- [18] BAI Guang-hui, TENG Wei, WANG Xiang-gang, QIN Jin-guo, XU Peng, LI Peng-cheng. Alkali desilicated coal fly ash as substitute of bauxite in lime-soda sintering process for aluminum production [J]. *Transactions of Nonferrous Metals Society of China*, 2010, 20(S): s169–s175.
- [19] YAO Z T, XIA M S, SARKER P K, CHEN T. A review of the alumina recovery from coal fly ash, with a focus in China [J]. *Fuel*, 2014, 120: 74–85.
- [20] LI Xiao-fei, YE Yu-zhen, XUE Sheng-guo, JIANG Jun, WU Chuan, KONG Xiang-feng, HARTLEY W, LI Yi-wei. Leaching optimization and dissolution behavior of alkali anions in bauxite residue [J]. *Transactions of Nonferrous Metals Society of China*, 2018, 28(6): 1248–1255.
- [21] LI Xiao-bin, ZHOU Zhao-yu, WANG Yi-lin, ZHOU Qiu-sheng, QI Tian-gui, LIU Gui-hua, PENG Zhi-hong. Enrichment and separation of iron minerals in gibbsitic bauxite residue based on reductive Bayer digestion [J]. *Transactions of Nonferrous Metals Society of China*, 2020, 30(7): 1980–1990.
- [22] CROKER D, LOAN M, HODNETT B K. Desilication reactions at digestion conditions: an in situ X-ray diffraction study [J]. *Crystal Growth and Design*, 2008, 8(12): 4499–4505.
- [23] SMITH P. The processing of high silica bauxites-Review of existing and potential processes [J]. *Hydrometallurgy*, 2009, 98: 162–176.
- [24] LI Xiao-bin, WANG Hong-yang, ZHOU Qiu-sheng, QI Tian-gui, LIU Gui-hua, PENG Zhi-hong, WANG Yi-lin. Efficient separation of alumina and silica in reduction-roasted kaolin by alkaline leaching [J]. *Transactions of Nonferrous Metals Society of China*, 2019, 29(2): 416–423.
- [25] LI Xiao-bin, WANG Hong-yang, ZHOU Qiu-sheng, QI Tian-gui, LIU Gui-hua, PENG Zhi-hong, WANG Yi-lin. Reaction behavior of kaolinite with ferric oxide during reduction roasting [J]. *Transactions of Nonferrous Metals Society of China*, 2019, 29(1): 186–193.
- [26] LI Xiao-bin, WANG Hong-yang, ZHOU Qiu-sheng, QI

- Tian-gui, LIU Gui-hua, PENG Zhi-hong. Efficient separation of silica and alumina in simulated CFB slag by reduction roasting-alkali leaching process [J]. Waste Management, 2019, 87: 798–804.
- [27] LI Xiao-bin, WANG Hong-yang, ZHOU Qiu-sheng, QI Tian-gui, LIU Gui-hua, PENG Zhi-hong. Phase transformation of hercynite during the oxidative roasting process [J]. JOM, 2020, 72(10): 3341–3347.
- [28] ZHENG Da, LU Hai-lin, SUN Xiu-yun, LIU Xiao-dong, HAN Wei-qing, WANG Lian-jun. Reaction mechanism of reductive decomposition of FGD gypsum with anthracite [J]. Thermochem Acta, 2013, 559: 23–31.

## 还原焙烧–碱浸工艺实现偏高岭石中氧化铝和氧化硅的分离： $\text{CaSO}_4$ 和 $\text{CaO}$ 的影响

王洪阳<sup>1,2</sup>, 张晓雪<sup>1</sup>, 杨思原<sup>1,2</sup>, 刘诚<sup>1,2</sup>, 罗立群<sup>1,2</sup>

1. 武汉理工大学 资源与环境工程学院, 武汉 430070;

2. 武汉理工大学 矿物资源加工与环境湖北省重点实验室, 武汉 430070

**摘要:** 采用循环流化床技术处理高铝煤矸石时会添加石灰石以起到固硫作用。此时, 循环流化床渣中的主要含钙矿物为  $\text{CaO}$  和  $\text{CaSO}_4$ , 含铝矿物为偏高岭石。研究  $\text{CaSO}_4$  和  $\text{CaO}$  对还原焙烧–碱浸工艺实现偏高岭石中氧化铝和氧化硅分离的影响。结果表明, 添加氧化铁还原焙烧可将偏高岭石完全转变为铝酸亚铁和二氧化硅固溶体(石英固溶体和方石英固溶体)。随后经碱浸可脱除还原焙烧产物中 95% 以上的二氧化硅。 $\text{CaSO}_4$  和  $\text{CaO}$  的添加可显著降低偏高岭石中氧化铝和氧化硅的分离效率, 其主要原因为含硅物相的形成: (1) 还原焙烧过程中生成铁橄榄石和钙长石; (2) 碱浸过程中铁橄榄石稳定存在, 而钙长石转变为方钠石和硅灰石。为实现循环流化床渣中氧化铝和氧化硅的综合提取, 高铝煤矸石中的硫应该在烟气中进行脱除, 而不适于在循环流化床燃烧过程中进行钙化固定。

**关键词:** 循环流化床渣; 偏高岭石; 含钙矿物; 还原焙烧; 碱浸

(Edited by Bing YANG)